Supplementary Information

Application of chiral cationic iridium(III) complexes for triplet-triplet annihilation up-conversion of photon energy in *R*-limonene

Akihiko Yamagishi,[a] Jun Yoshida [b] and Hisako Sato* [c]

[a] Faculty of Medicine, Toho University, Ota-ku 143-8540, Japan

[b] Department of Chemistry, College of Humanities & Sciences, Nihon University, Tokyo 156-8550, Japan

[c] Faculty of Science, Ehime University, Matsuyama, Ehime 790-8577, Japan

Contents

1. Chromatographic resolution and electronic circular dichroism spectra of $[Ir(piq)_2(C_{19}bpy)]PF_6$

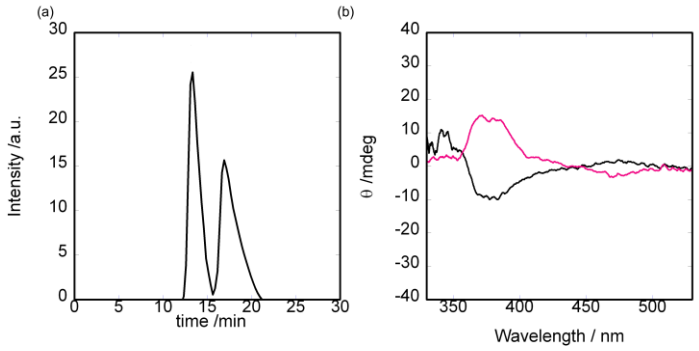

Figure S1. (a) Chromatogram when racemic $[Ir(piq)_2(C_{19}bpy)]PF_6$ was eluted on a HPLC column (CHIRALPACK IA (Daicel, Japan)). Elution conditions were following; flow rate (1.0 $mLmin^{-1}$), wavelength (340 nm), eluent (acetonitrile containing 0.1 (v/v) % of diethylamine and 0.1 (v/v) % of trifluoroacetic acid, and temperature (27°C). The first and second peaks were Δ- and Λ-enantiomers, respectively.

(b) The electronic circular dichroism spectra of the resolved enantiomers of $[Ir(piq)_2(C_{19}bpy)]PF_6$ in a mixture of *R*-limonene and acetonitrile (black and red curves for Δ- and Λ-enantiomers, respectively). Samples were prepared by mixing the samples used for TTA-UC experiments (0.5 mL) with acetonitrile (2.0 mL).

2. Electronic circular dichroism spectra of enantiomeric $[Ir(piq)_2(dmbpy)]PF_6$ and $[Ir(piq)_2(C_9bpy)]PF_6$

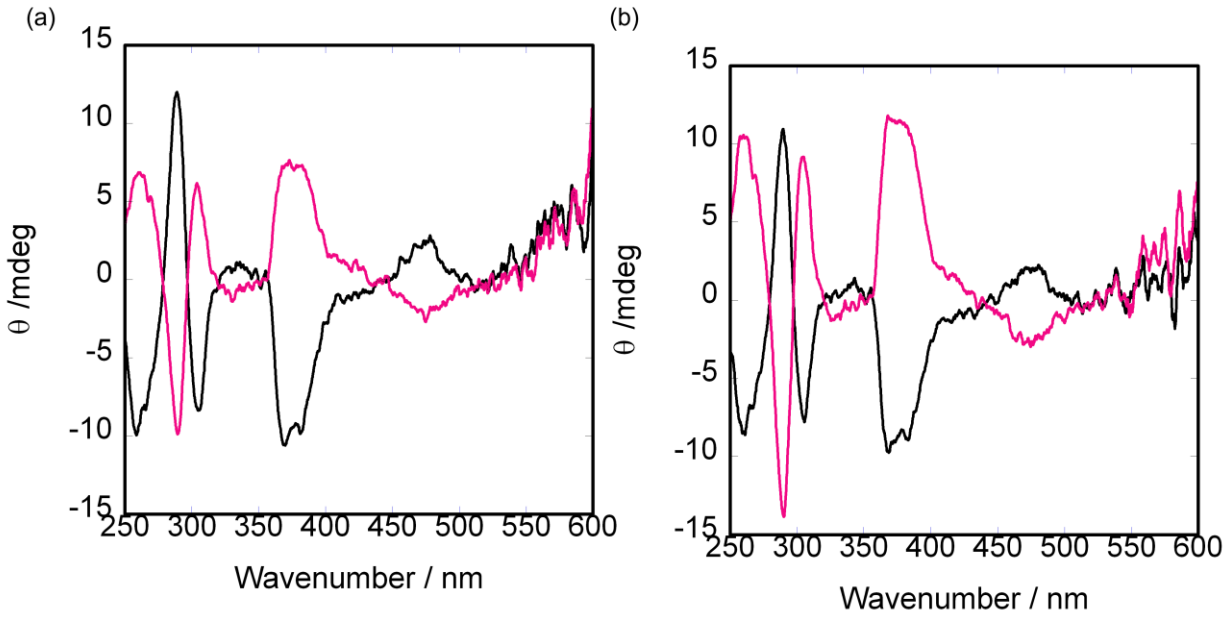

Figure S2. Electronic circular dichroism spectra of (a) $[Ir(piq)_2(dmbpy)]PF_6$ (in methanol) and (b) $[Ir(piq)_2(C_9bpy)]PF_6$ (in methanol). The black and red curves are for Δ– and Λ–enantiomers, respectively.

3. Solubility of racemic and enantiomeric $[Ir(piq)_2(dmbpy)]PF_6$ in *R*-limonene

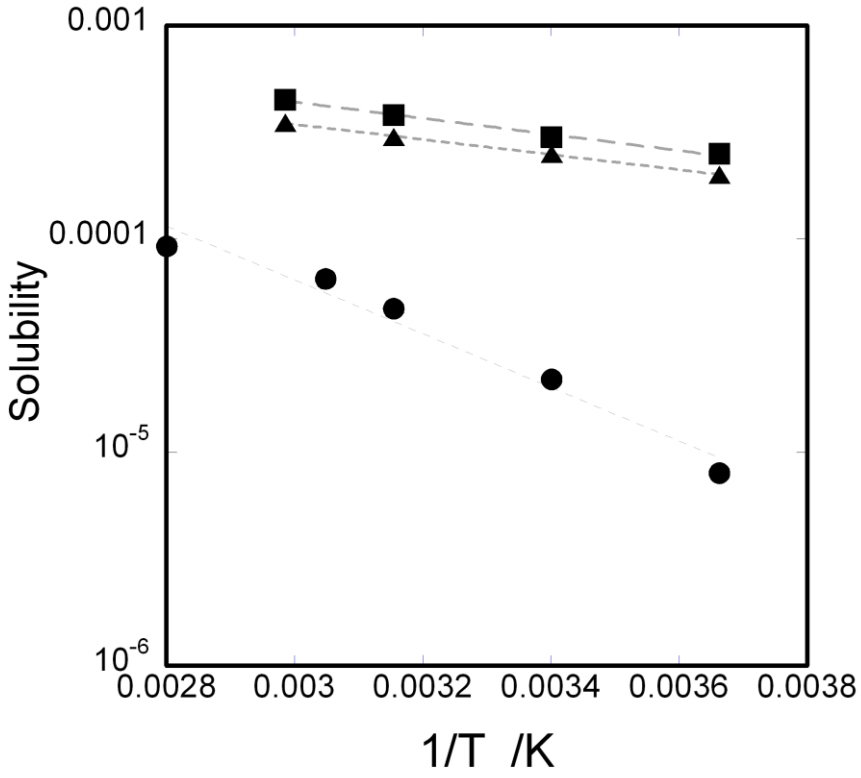

Figure S3. Temperature dependence of solubility of racemic (filled circle), Δ- (filled triangle) and Λ-$[Ir(piq)_2(dmbpy)]PF_6$ (filled square) in *R*-limonene. From the slope of each plot, the enthalpy of solubilization (-ΔH) was calculated to be 24.1, 6.8 and 7.2 $kJmol^{-1}$, respectively, according to the equation of (slope) = ΔH/*R* (*R* = gas constant).

4. Emission spectra when a laser light was irradiated onto an *R*-limonene solution containing Ir(III) complex and DPA

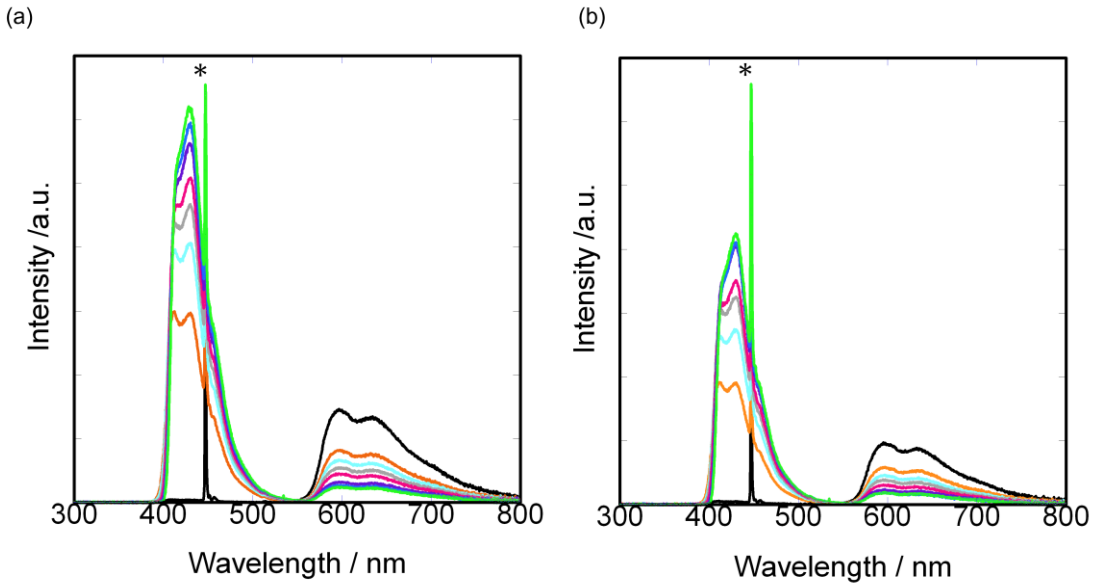

Figure S4. A laser light was irradiated onto a *R*-limonene solution containing DPA and (a) Δ- or (b) Λ-$[Ir(piq)_2(dmbpy)]^+$ under air, respectively. The concentration of DPA was 0 mM (black), 0.32 mM (orange), 0.63 mM (sky-blue), 0.92 mM (grey), 1.2 mM (red), 1.7 mM (violet), 2.2 mM (blue) and 2.6 mM (green), respectively. The concentration of Ir(III) complex was 2.4×10^{-5} M or 1.8×10^{-5} M for Δ- or Λ-$[Ir(piq)_2(dmbpy)]^+$, respectively. A scattered fraction of a laser light is indicated by *(asterisk).

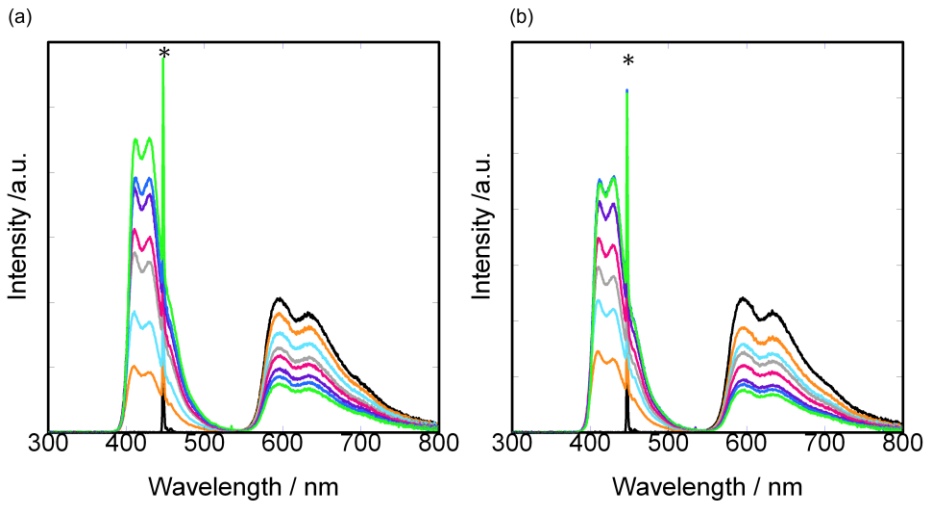

Figure S5. A laser light was irradiated onto a *R*-limonene solution containing DPA and (a) Δ-or (b) Λ-$[Ir(piq)_2(C_9bpy)]^+$ under air, respectively. The concentration of DPA was 0 mM (black), 0.08 mM (orange), 0.16 mM (sky-blue), 0.23 mM (grey), 0.30 mM (red), 0.43 mM (violet), 0.55mM (blue) and 0.66 mM (green), respectively. The concentration of Ir(III) complex was 2.7×10^{-5} M or 2.9×10^{-5} M for Δ- or Λ-$[Ir(piq)_2(C_9bpy)]^+$, respectively. A scattered fraction of a laser light is indicated by *(asterisk).

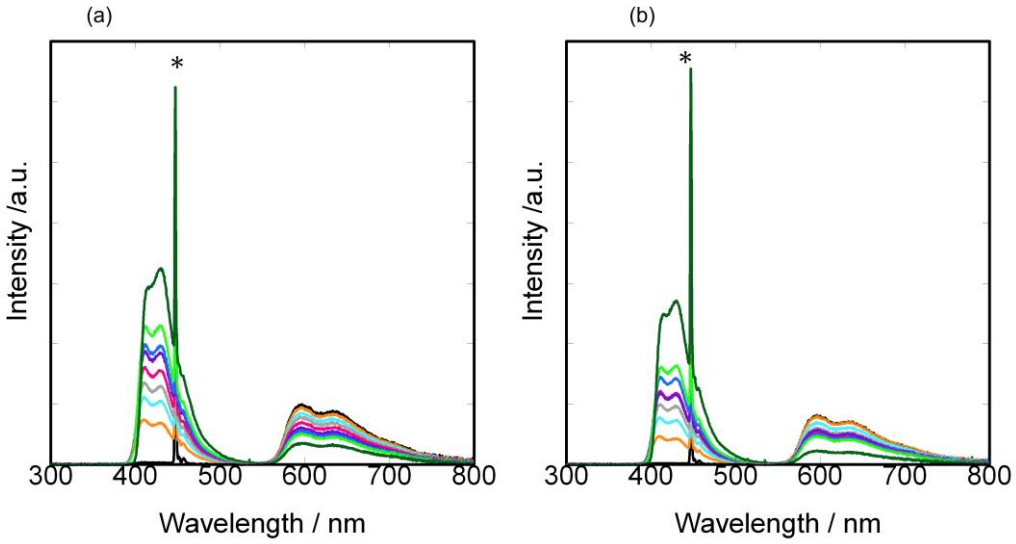

Figure S6. A laser light was irradiated onto a *R*-limonene solution containing DPA and (a) Δ- or (b) Λ-$[Ir(piq)_2(C_{19}bpy)]^+$ under air, respectively. The concentration of DPA was 0 mM (black), 0.08 mM (orange), 0.15 mM (sky-blue), 0.22 mM (grey), 0.29 mM (red), 0.41mM (violet), 0.52 mM (blue), 0.63mM (light green) and 1.26 mM(moss green), respectively. The concentration of Ir(III) complex was 1.5×10^{-5} M or 1.3×10^{-5} M for Δ- or Λ-$[Ir(piq)_2(C_{19}bpy)]^+$, respectively. . A scattered fraction of a laser light is indicated by *(asterisk).

5. S-V plots of *R*-limonene solutions containing DPA and $[Ir(piq)_2(C_nbpy)]^+$(n= 9 or 19)

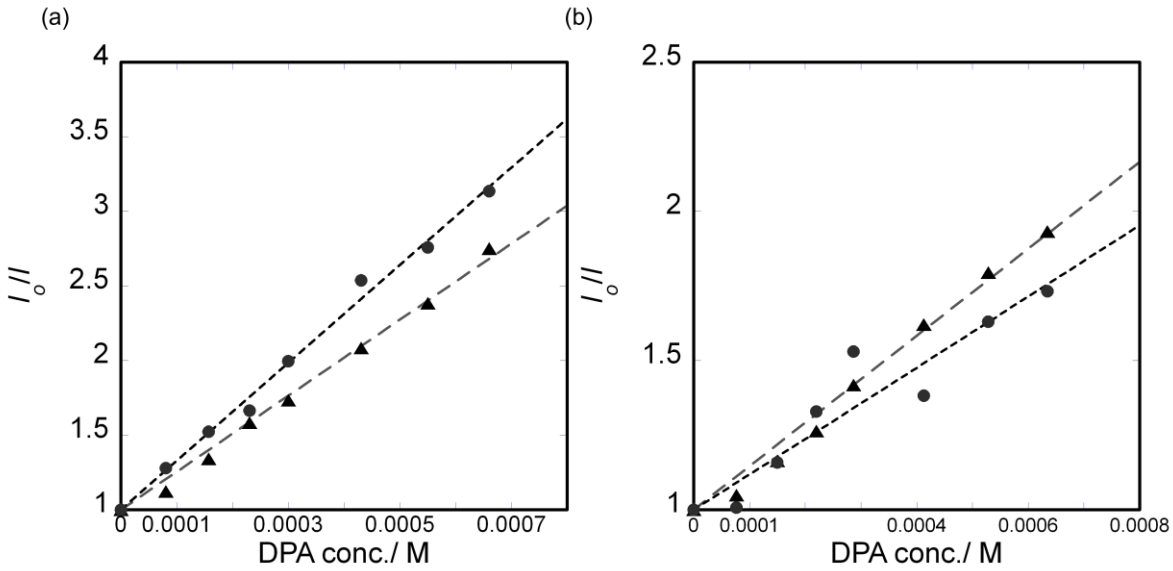

Figure S7. S-V plots of Δ-or Λ-$[Ir(piq)_2(C_9bpy)]^+$ (a) and Δ-or Λ-$[Ir(piq)_2(C_{19}bpy)]^+$ (b) as an emitter and DPA as a quencher. Plots of solid triangles and solid circles are for Δ- and Λ-enantiomers, respectively. Experimental conditions are described in the text.

6. UV-vis spectra of $[Ir(piq)_2(dmbpy)]PF_6$, $[Ir(piq)_2(C_nbpy)]PF_6$ (n=9, 19) and DPA alone in *R*-limonene

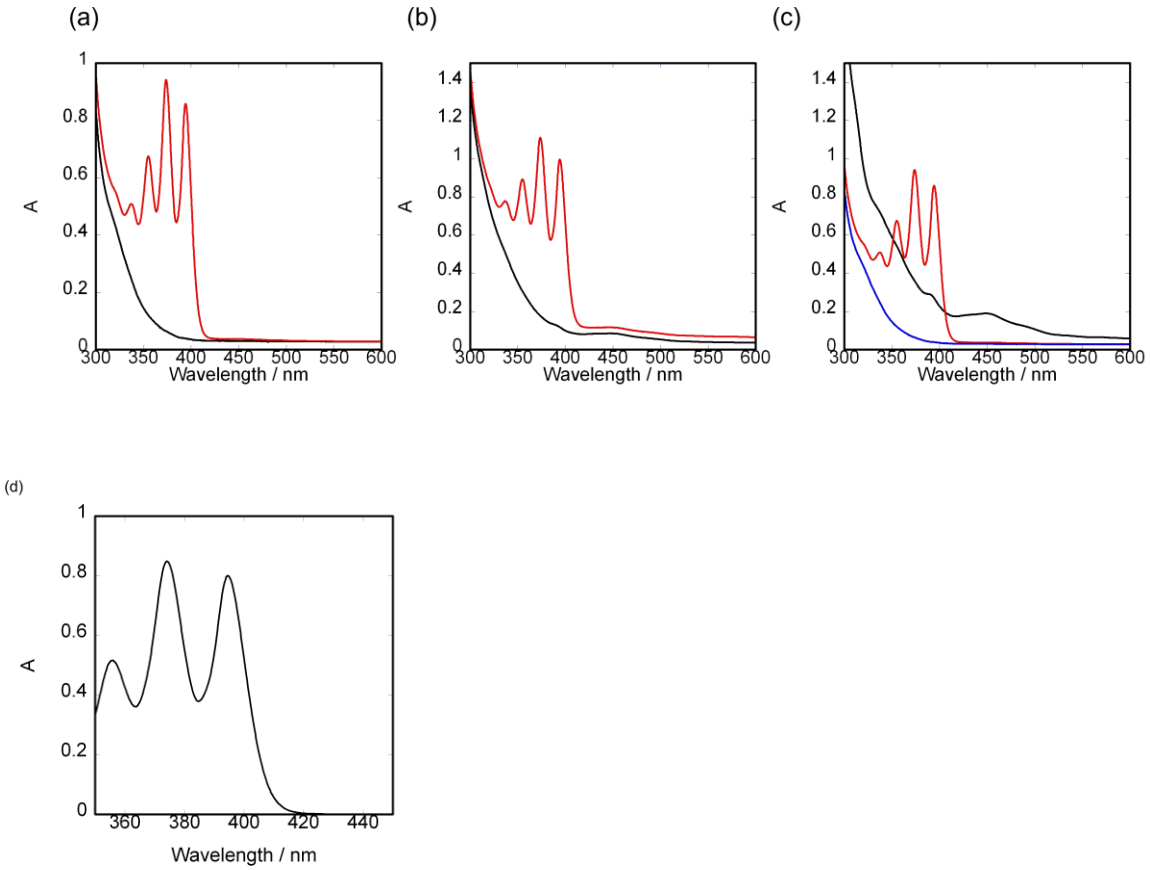

Figure S8. UV-vis spectra of (a) Δ-$[Ir(piq)_2(dmbpy)]^+$ (4.0×10^{-6} M) and DPA (8.0×10^{-6} M), (b) Δ-$[Ir(piq)_2(C_9bpy)]$ (6.9×10^{-5} M) and DPA (6.9×10^{-5} M), (c) Δ-$[Ir(piq)_2(C_{19}bpy)]^+$ (4.0×10^{-6} M) and DPA (6.9×10^{-5} M) and (d) DPA (6.9×10^{-5} M). A medium was *R*-limonene (blue line in (c)). The spectra were measured using a quartz cell of 2 mm optical path.
The black and red lines are for Ir(III) complex only and for a pair of Ir(III) complex/DPA, respectively.

7. Lifetimes of $[Ir(piq)_2(dmbpy)]PF_6$ and $[Ir(piq)_2(Cnbpy)]PF_6$ (n=9, 19) in *R*-limonene

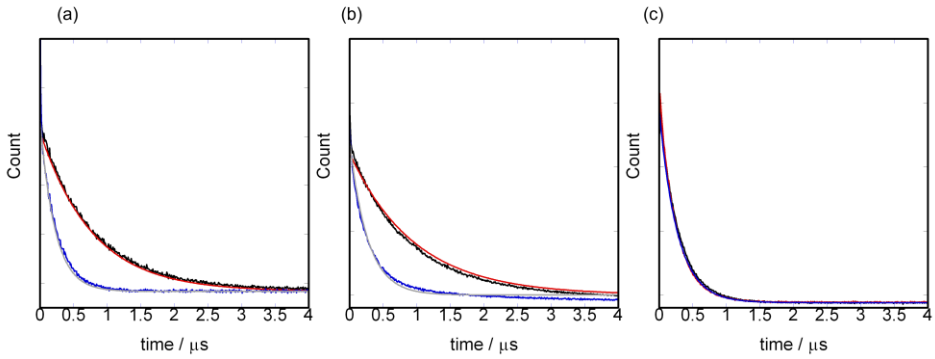

Figure S9. Decay curves of (a) Δ-$[Ir(piq)_2(dmbpy)]PF_6$, (b) Δ-$[Ir(piq)_2(C_9bpy)]$ PF_6 and (c) Δ-$[Ir(piq)_2(C_{19}bpy)]$ PF_6 in *R*-limonene. Emission was measured at 600 nm, when the sample solutions were irradiated with a laser pulse at 355 nm. Blue and grey lines are the observed and fitting curves under air, respectively. Black and red lines are the observed and fitting curves under nitrogen atmosphere, respectively. Fitting was performed under the assumption of a single exponential decay. The results are summarized in Table S1.

Table S1. Emission lifetimes in *R*-limonene

Ir(III) complex	Lifetime under air (μs)	Lifetime under N_2 (μs)
Δ-$[Ir(piq)_2(dmbpy)]^+$	0.22	0.78
Δ-$[Ir(piq)_2(C_9bpy)]$	027	0.97
Δ-$[Ir(piq)_2(C_{19}bpy)]^+$	0.28	0.28

8. Emission spectrum of a CH_2Cl_2 solution of $[Ru(dmbpy)_3]Cl_2$ and DPA as a standard

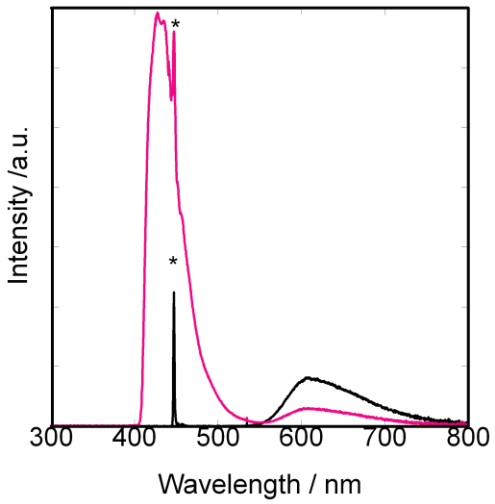

Figure S10. A laser light was irradiated onto a CH_2Cl_2 solution containing $[Ru(dmbpy)_3]Cl_2$ alone (black) or $[Ru(dmbpy)_3]Cl_2$ and DPA (red), respectively. The measurements were performed under air. The concentrations of $[Ru(dmbpy)_3]Cl_2$ and DPA was 0.28 mM and 6.4 mM, respectively. A scattered fraction of a laser light is indicated by *(asterisk).

9. Laser intensity dependence of up-conversion efficiency for an *R*-limonene solution containing Λ-[Ir(piq)$_2$(dmbpy)] and DPA

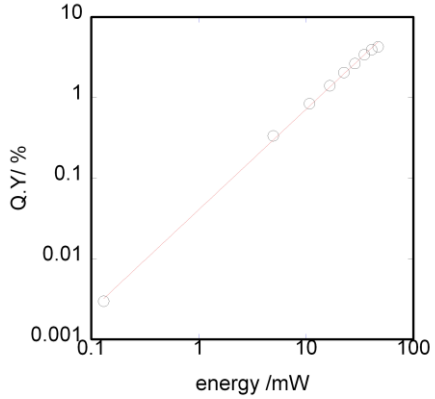

Figure S11. The dependence of TTA-UC quantum yield on the laser light power. The sample was a *R*-limonene containing Λ-[Ir(piq)$_2$(dmbpy)] (1.8×10^{-5} M) and DPA (2.6 mM).